did not obtain work of formation results for cavities substantially larger than the solvent molecules, and that constitutes the chief limitation on the conclusions that are drawn here. Calculations of cavity works for much larger cavities will require alternative methods.

Acknowledgment. We thank Michael A. Wilson for help in acquisition of some of the data. This work was supported in part by NASA-Ames-UC Berkeley Intergovernmental Personnel Exchange Agreement NCA-2 315 and by the Numerical Aerodynamics Simulation (NAS) program.

Photoinduced Electron Transfer in Self-Associated Complexes of Several Uroporphyrins and Cytochrome *c*

J. S. Zhou, E. S. V. Granada, N. B. Leontis, and M. A. J. Rodgers*

Contribution from the Center for Photochemical Sciences, Bowling Green State University, Bowling Green, Ohio 43403. *Received November 13, 1989*

Abstract: Photoinduced electron transfer between cytochrome *c* and free base and metallouroporphyrin (Up, MUp) has been studied. Difference absorption spectrophotometry showed that the electrostatic interactions between Up and cytc(III) result in their forming a self-associated 1:1 complex in the ground state with a binding constant that depends upon the ionic strength. In the complex, the photoexcited uroporphyrin singlet state was quenched through a static interaction with the protein. Even under the most favorable quenching conditions, i.e., when all porphyrin was complexed, residual fluorescence was noted. More significantly the excited singlet state of the complex was shown to undergo small, but significant, intersystem crossing. These triplet states rapidly underwent an electron-transfer process that yielded transiently the Fe(II) form of the protein. This is the first observation of such a process from a porphyrin/cytochrome self-association complex. Both the rates of bimolecular electron transfer between uncomplexed partners and intramolecular electron transfer from the uroporphyrin triplet to cytochrome *c*, as well as the thermal intramolecular back-reaction, have been measured by transient kinetic spectroscopy. The rate constants of intramolecular electron transfer for zinc uroporphyrin/cytochrome *c* and zinc cytochrome *c*/ferriuroporphyrin have been also determined. These three couples allow us to estimate approximately the reorganization energy λ in the semiclassical electron-transfer theory.

It is now well-known that biological energy is channeled through the photosynthetic and mitochondrial respiratory chain via electron-transfer reactions.[1-5] This has stimulated a variety of studies, especially on fixed-site electron transfer in proteins, in an attempt to understand long-range electron-transfer reactions in biological systems. In recent years, mitochondrial cytochrome *c* has been one of the proteins most widely used as the study system,[6] since it is well characterized in terms of both primary and tertiary structure and since X-ray crystallographic structures are available for a number of native cytochrome *c* systems, thereby facilitating model building.[7] The approaches applied by a number of research groups to fix electron-transfer reaction centers at given distances in cytochrome *c* systems are either to covalently bond a donor and/or acceptor residue to specified sites on the cytochrome *c* surface[8-14] or to rely on electrostatic self-association between cytochrome *c* and its partner.[15-22]

On the basis of these concepts, we decided to study cytochrome *c*, which has six cationic lysine residues at its surface near the solvent-exposed heme site, and as redox partner use uroporphyrin, which has eight carboxylate residues on short side chains disposed around the periphery. Our hypothesis was that this pair would form an electrostatic self-associated complex in aqueous solution that could perhaps be induced to undergo electron transfer when the porphyrin was excited into its triplet state. This resembles the system employed by Cho et al.[23] who used cytochrome *c*

(1) Chance, B., DeVault, D. C., Frauenfelder, H., Marcus, R. A., Schrieffer, J. R., Sutin, N., Eds. *Tunneling in Biological Systems*; Academic Press: New York, 1979.
(2) Hatefi, Y. *Annu. Rev. Biochem.* **1985**, *54*, 1015.
(3) Dixit, B. P. S. N.; Vanderkooi, J. M. *Curr. Top. Bioenerg.* **1984**, *13*, 159.
(4) Michel-Beyerle, M. E., Ed. *Antennas and Reaction Centers of Photo-Synthetic; Bacteria*; Springer-Verlag: Berlin, 1985.
(5) Govindjee, Ed. *Photosynthesis. Energy Conversion by Plants and Bacteria*; Academic Press: New York, 1982; Vol. 1.
(6) Pielak, G. J.; Concar, D. W.; Moor, G. R.; Williams, R. J. P. *Protein Eng.* **1987**, *1*, 83-88.
(7) Takano, T.; Dickerson, R. E. *J. Mol. Biol.* **1981**, *153*, 79-94. Takano, T.; Dickerson, R. E. *J. Mol. Biol.* **1981**, *153*, 95-115. Ochi, H.; Hata, Y.; Tanaka, N.; Kakudo, M.; Sakurai, T.; Aihara, S.; Morita, Y. *J. Mol. Biol.* **1983**, *166*, 407-418.
(8) Crutchley, R. J.; Ellis, W. R.; Gray, H. B. *J. Am. Chem. Soc.* **1985**, *107*, 5092-5094.
(9) Mayo, S. L.; Ellis, W. R.; Crutchley, R. J.; Gray, H. B. *Science* **1986**, *233*, 948-952.
(10) Bechtold, R.; Gardineer, M. B.; Kazmi, A.; Van Hemelryck, B.; Isied, S. S. *J. Phys. Chem.* **1986**, *90*, 3800-3804.
(11) Bechtold, R.; Kuehn, C.; Lepre, C.; Isied, S. S. *Nature* **1986**, *322*, 286-288.
(12) Elias, H.; Chou, M. H.; Winkler, J. R. *J. Am. Chem. Soc.* *110*, **1988**, 429-434.
(13) Conrad, D. W.; Scott, R. A. *J. Am. Chem. Soc.* **1989**, *111*, 3461-3463.
(14) Meade, T. J.; Gray, H. B.; Winkler, J. R. *J. Am. Chem. Soc.* **1989**, *111*, 4353-4356.
(15) Ho, P. S.; Sutoris, C.; Liang, N.; Maragoliash, E.; Hoffman, B. M. *J. Am. Chem. Soc.* **1985**, *107*, 1070-1071.
(16) Cheung, E.; Taylor, K.; Kornblatt, J. A.; English, A. M.; McLendon, G.; Miller, J. R. *Proc. Natl. Acad. Sci. U.S.A.* **1986**, *83*, 1330-1333.
(17) Liang, N.; Kang, C. H.; Ho, P. S.; Maragoliash, E.; Hoffman, B. M. *J. Am. Chem. Soc.* **1986**, *108*, 4665-4566.
(18) McLendon, G.; Miller J. R. *J. Am. Chem. Soc.* **1985**, *107*, 7811-7816.
(19) Conklin, K. T.; McLendon, G. *J. Am. Chem. Soc.* **1988**, *110*, 3345-3350.
(20) Hazzard, J. T.; Poulos, T. L.; Tollin, G. *Biochemistry* **1987**, *26*, 2836-2848.
(21) Hazzard, J. T.; McLendon, G.; Cusanovich, M. A.; Tollin, G. *Biochem. Biophys. Res. Commun.* **1988**, *151*, 429-434.
(22) Cheddar, G.; Meyer, T. E.; Cusanovich, M. A.; Stout, C. D.; Tollin, G. *Biochemistry* **1989**, *28*, 6318-6322.

0002-7863/90/1512-5074$02.50/0

Table I. Half-Cell Redox Potentials vs NHE (25 °C)

redox couple	$\Delta E°$ (V)	redox couple	$\Delta E°$ (V)
cytc(III)/cytc(II)	0.26[a]	$Fe^{III}Up(Cl)/Fe^{II}Up(Cl)$	−0.43
$Zncytc^+/^3Zncytc^*$	−0.88[b]	$Zncytc^+/Zncytc$	0.80[b]
$ZnUp^+/^3ZnUp^*$	−0.93[c]	$ZnUp^+/ZnUp$	0.83[c]
$Up^+/^3Up^*$	−0.80[d]	Up^+/Up	0.86[d]

[a] Reference 28. [b] Reference 29. [c] Reference 26. [d] Estimated value from that of octaethylporphyrin (see text).

together with anionic and cationic meso-substituted tetraphenylporphyrins. However, they reported only bimolecular electron transfer between freely diffusing partners. They did not observe electron transfer within a self-associated complex. In this report we demonstrate that for couples of uroporphyrin/cytochrome *c*, zinc uroporphyrin/cytochrome *c*, and zinc cytochrome *c*/ferriuroporphyrin such self-association occurs and when photoexcited results in rapid forward and reverse electron transfer. Thus, the interacting system provides a molecular framework within which the electron donor and acceptor sites are fixed.

Experimental Section

Materials. Horse heart cytochrome *c*, Type VI (cytc(III)), was purchased from Sigma Chemical Co. The reduced form was converted to the oxidized form by addition of excess $K_3Fe(CN)_6$ followed by extensive dialysis against appropriate buffers. The concentration of cytochrome *c* was determined on the basis of $\epsilon_{528} = 11\,200\ M^{-1}\ cm^{-1}$.[24] Uroporphyrin I dihydrochloride (Up) was obtained from Porphyrin Products Inc. and used as received without further purification. Zinc cytochrome *c* was prepared following the procedure of Conklin and McLendon.[19]

The metallouroporphyrin ($Zn^{II}Up$ and $Fe^{III}Up(Cl)$) was prepared by addition of excess metal acetate to a solution of the free base uroporphyrin in glacial acetic acid. The solution was then heated to 60 °C for 24 h. After cooling, the solvent was removed under reduced pressure and the dark solid was dissolved in base solution. The solution was filtered and acidified with HCl. The precipitate was washed with dilute HCl solution (pH 1.5) and dried under vacuum. The purity was checked by visible absorption spectroscopy, and fluorescence showed no residual free-base uroporphyrin present. In the case of $Fe^{III}Up(Cl)$, the ferro acetate was obtained by dissolving iron wire in glacial acid under N_2 stream.

All solutions were prepared with distilled water purified by a Barnstead NANOpure II water purification system. The sodium phosphate buffer (pH 7.26, 10 mM ionic strength) was prepared with molecular biology reagent grade monobasic and dibasic sodium phosphate (Sigma). Ionic strengths higher than 10 mM were obtained by adding NaCl; those lower than 10 mM, by dilution.

Methods. Spectrophotometric measurements were performed on a Perkin-Elmer UV/vis 3840 Lambda Array spectrophotometer, with a thermostated cell holder, interfaced to a Princeton microcomputer. Difference spectra, Job plots, and spectrophotometric titrations were obtained by the method of Erman and Vitello,[25] with a tandem mixing cell (Uvonic Instruments, Inc.) at 25 °C.

Steady-state fluorescence quenching studies were carried out at 25 °C on a Spex Fluorolog 2 Series spectrofluorimeter with a thermostated cell holder. The excitation wavelength (612 nm) was chosen so that the absorbance ranged from 0.1 to 0.2 and that the fraction of light absorbed by Up was predominant over the region of cytc(III) concentration covered. The emission intensities were measured by integrating the fluorescence spectrum between 650 and 750 nm and then by normalizing to the absorbance of Up at the excitation wavelength.

The redox potential of $Fe^{III}Up(Cl)$ in water was determined by the cyclic voltammetric method with the aid of a EG&G Princeton Applied Research Model 173 potentiostat. An aqueous saturated calomel electrode was used as reference electrode, and a hanging-drop mercury electrode was used as the working electrode for reduction. Kalyanasundaram et al. have estimated the oxidation potential for ZnUp in ground and excited states.[26] According to their studies, the redox potentials of the uroporphyrin are almost identical with those of the octaethylporphyrin. So, we have estimated the oxidation potential of Up from that of the octaethylporphyrin.[27] The potentials (vs NHE at 25 °C) for

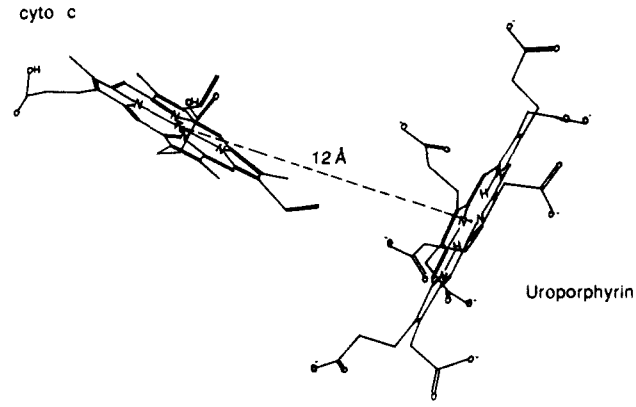

Figure 1. Model of the complex formed between cytochrome *c* and uroporphyrin based on the computer-generated complex model (see text for details).

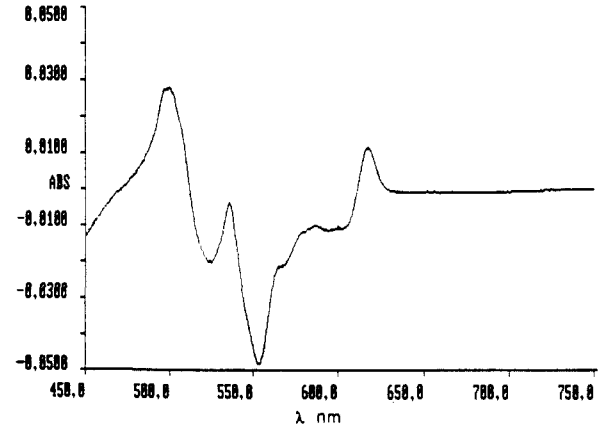

Figure 2. Difference spectrum obtained by subtraction of the spectrum after mixing (the uroporphyrin/cytochrome *c* complex) from that before mixing (the sum of the uroporphyrin and cytochrome *c* spectra), with a tandem mixing cell. The final concentrations of uroporphyrin and cytochrome *c* are 17.5 μM (25 °C, pH 7.26, and 4 mM ionic strength in phosphate buffer).

compounds involved in this electron-transfer study are collected in Table I.

Electron-transfer kinetics derived from triplet states were performed by laser flash kinetic spectrophotometry with the 532-nm output of a Q-switched Quantel YG 571-C10 Nd:YAG laser as the excitation source, described elsewhere.[30] The reaction rates were measured as a function of cytochrome *c* concentrations (5–50 μM) at constant uroporphyrin concentration (35 μM) in phosphate buffer at various ionic strengths (4–500 mM) under anaerobic conditions. In the case of ZnUp/cytc(III) and $Zncytc/Fe^{III}Up(Cl)$, the concentration (10 μM) of electron donor was used while that of electron acceptor was varied between 5 and 30 μM at 4 mM ionic strength.

Computer Graphics. Computer graphics experiments were carried out with the use of MACROMODEL (the Columbia Chemistry Molecular Modeling System) program running on VAX8530 with an Evans & Sutherland PS390 computer graphics system. The coordinates for horse heart cytochrome *c* were derived from the closely related molecule tuna cytochrome *c*,[31] whose coordinates were obtained from the Brookhaven Protein Data Bank.[32] The uroporphyrin molecular structure was drawn with the Macromodel computer graphics system and further refined by

(23) Cho, K. C.; Che, C. M.; Ng, K. M.; Choy, C. L. *J. Am. Chem. Soc.* **1986**, *108*, 2814–2818.
(24) Maragoliash, E.; Frohwirt, N. *Biochem. J.* **1959**, *71*, 570–572.
(25) Erman, J. E.; Vitello, L. B. *J. Biol. Chem.* **1980**, *255*, 6224–6227.
(26) Kalyanasundaram, K.; Shelnutt, J. A.; Gratzel, M. *Inorg. Chem.* **1988**, *27*, 2820–2825.
(27) Felton, R. H. In *The Porphyrins*: Dolphin, D., Ed.; Academic: New York, 1978, Vol. V, Part C.
(28) Armstrong, F. A.; Hill, H. A. O.; Walton, N. J. Q. *Rev. Biophys.* **1986**, *18*, 261–322.
(29) Magner, E.; McLendon, G. *J. Phys. Chem.* **1989**, *20*, 7130–7134.
(30) Rodgers, M. A. J. In *Primary Photo-Process in Biology and Medicine*; Bensasson, R. V., Jori, G., Land, E. J., Truscott, T. G., Eds.; Plenum: New York, 1985; pp 1–23.
(31) Swanson, R.; Trus, B. L.; Mandel, N.; Mandel, G.; Kallai, O.; Dickerson, R. E. *J. Biol. Chem.* **1977**, *252*, 759–775.
(32) Bernstein, F. C.; Koetzle, T. F.; Williams, G. T. B.; Meyer, E. F., Jr.; Brice, M. D.; Rodgers, J. R.; Kennard, O.; Schimanouchi, T.; Tasume, M. *J. Mol. Biol.* **1977**, *112*, 535–542.

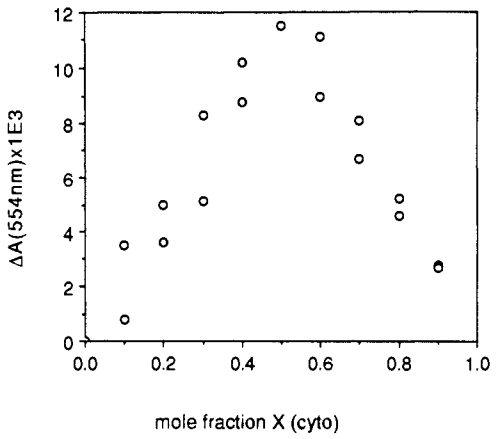

Figure 3. Job plot of the change in absorbance at 554 nm as a function of the mole fraction of cytc(III). The total concentration of the two compounds was held constant at 8.75 μM (25 °C, pH 7.26, and 4 mM ionic strength in phosphate buffer).

Table II. Binding Constants at Different Ionic Strengths (25 °C)

μ (mM)	K_A (M^{-1})
4	$(9.5 \pm 1.5) \times 10^5$
20	$(5.4 \pm 1) \times 10^4$
60	$(1.1 \pm 1) \times 10^4$

minimizing the molecular energy to get rMS derivative ≤0.005 kJ/A.

The model of the complex was obtained by optimization of electrostatic interactions between positively charged lysine residues (Lys 13, Lys 27, Lys 72, Lys 79) around the perimeter of the cytochrome *c* heme crevice and the negatively charged acidic groups of uroporphyrin and steric interactions on the interface between the two partners. This was achieved by following the procedure of Simondsen et al.[33]

Results

1. Computer Modeling. Figure 1 shows the uroporphyrin/cytochrome *c* complex structure modeled by optimizing electrostatic and steric interactions between the two molecules. The estimated center–center and edge–center distances are ca. 12 and 7.8 Å, respectively. The two tetrapyrrole rings are approximately perpendicular.

2. Ground-State Complex. The difference spectrum in the visible region that results from the interaction of cytochrome *c* with uroporphyrin is shown in Figure 2. The maximal absorbance change (ΔA) of the spectrum (at 554 nm) was monitored to determine the stoichiometry of the complex and its stability. The Job plot shown in Figure 3 indicates that the observed difference spectrum arises from the predominent formation of a 1:1 self-association complex between cytochrome *c* and uroporphyrin. This finding is substantiated by titration curves. This result is consistent with the result of Clark-Ferris and Fisher,[34] They found an electrostatically stabilized 1:1 complex between cytochrome *c* and *meso*-tetrakis(4-carboxyphenyl)porphyrin.[34] Based on this fact of 1:1 complex formed between Up and cytc(III), the change of ΔA as a function of cytc(III) concentration at constant concentration of Up should be described by the quadratic equation

$$\Delta A = ([\mathrm{Up}]_0 + [\mathrm{cytc}]_0) + 1/K_A - \{([\mathrm{Up}]_0 + [\mathrm{cytc}]_0 + 1/K_A)^2 - 4[\mathrm{Up}]_0[\mathrm{cytc}]_0\}^{1/2}\Delta A_\infty/2[\mathrm{Up}]_0$$

Titration data were fitted with a nonlinear regression program (NCSS) to determine binding constants. The dependencies of the binding constant K_A on ionic strength as determined from titration curves are shown in Table II.

3. Fluorescence Quenching. A study of the quenching of uroporphyrin fluorescence by cytochrome *c* was carried out at pH 7.26 and at different ionic strengths (4, 20, 60, and 500 mM),

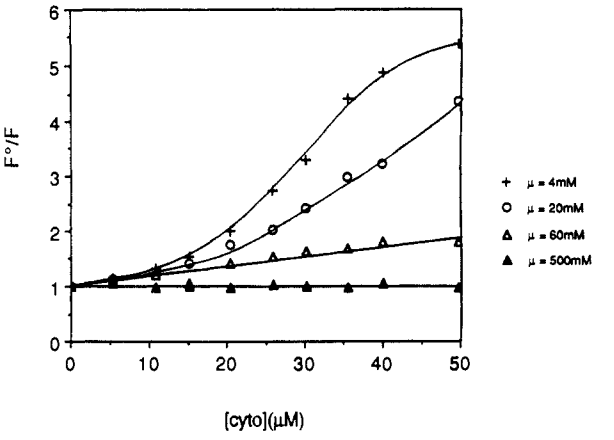

Figure 4. Normalized integrated fluorescence intensity ratio F^0/F as a function of cytochrome *c* concentration at 25 °C, pH 7.26, and at different ionic strengths.

The results (Figure 4) show that there is efficient quenching at low ionic strength, but the Stern–Volmer plot is nonlinear with upward curvature, indicating ground-state complex formation. A linear relationship is found at 60 mM ionic strength, while no quenching was noted at 500 mM ionic strength over the concentration range covered. At the lowest ionic strength (4 mM), the Stern–Volmer plot levels out at high cytochrome *c* concentration, indicating a low (ca. 10%) level of unquenched fluorescence.

4. Triplet-State Kinetics. a. High Ionic Strength. At μ = 500 mM, ground-state complexation between Up and cytc(III) was greatly reduced through charge-screening effects. Irradiation of an aqueous solution of Up with a 10-ns pulse of 532-nm light gave rise to the rapid appearance (<100 ns) of the T_1 state of Up having an apparent absorption maximum near 440 nm. In argon-saturated solution this species had a lifetime of 0.6 ms, being quenched rapidly in air-saturated solution. When cytc(III) was added, the Up(T_1) state was quenched with purely exponential kinetics with a rate that was first order in cytochrome *c* concentration. Concomitant with this cytc(III)-induced decay, we observed the delayed formation of new absorbances near 550 and 606 nm (Figure 5) where cytc(II) and Up^+ species absorb respectively. These formation rates showed behavior identical with the T_1 decay (Figure 6) monitored at 434 nm, the isosbestic point for the cytc(III)/cytc(II) absorbances. A bimolecular rate constant for the reaction of 4.1×10^8 M^{-1} s^{-1} was extracted from the slope of Figure 6.

In another series of experiments we used the complete-conversion method to evaluate a value of $\Delta\epsilon_{434} = 4.2 \times 10^4$ M^{-1} cm^{-1} for Up(T_1). Together with the literature value of 1.85×10^4 M^{-1} cm^{-1} [24] for the Fe(III) to Fe(II) conversion in cytochrome *c*, we evaluated

$$\Delta\epsilon_T(\mathrm{Up})/\Delta\epsilon_{550}(\mathrm{cytc}) = 2.3$$

From Figure 6 we note that at 40 mM cytc(III) the decay of Up(T_1) by quenching far exceeds that of the intrinsic decay; i.e., >95% of all triplets are being quenched. However, under these conditions we found a ratio of the absorbances of the T_1 and cytc(II) species, extrapolated to zero time, was ca. 10.3. Since

$$[T_1]/[\mathrm{cytc(II)}] = [\Delta A_T(\mathrm{Up})/\Delta A_{550}(\mathrm{cyt})]/[\Delta\epsilon_T(\mathrm{Up})/\Delta\epsilon_{550}(\mathrm{cytc})]$$

it follows that

$$[T_1]/[\mathrm{cytc(II)}] = 10.3/2.3 = 4.5$$

i.e., only ca. 22% of the initial T_1 states shows up as cytc(II) species, even under optimal quenching conditions.

b. Low Ionic Strength (4 mM). (1) Uroporphyrin and Cytc(III). At low ionic strengths the decay of Up(T_1) in the absence of cytc(III) produced by 532-nm laser excitation in argon-saturated solutions was exponential with a lifetime of 2 ms. When cytc(III)

(33) Simondsen, R. P.; Weber, P. C.; Salemme, F. R.; Tollin, G. *Biochemistry* **1982**, *21*, 6366–6375.
(34) Clark-Ferris, K. K.; Fisher, J. *J. Am. Chem. Soc.* **1985**, *107*, 5007–5008.

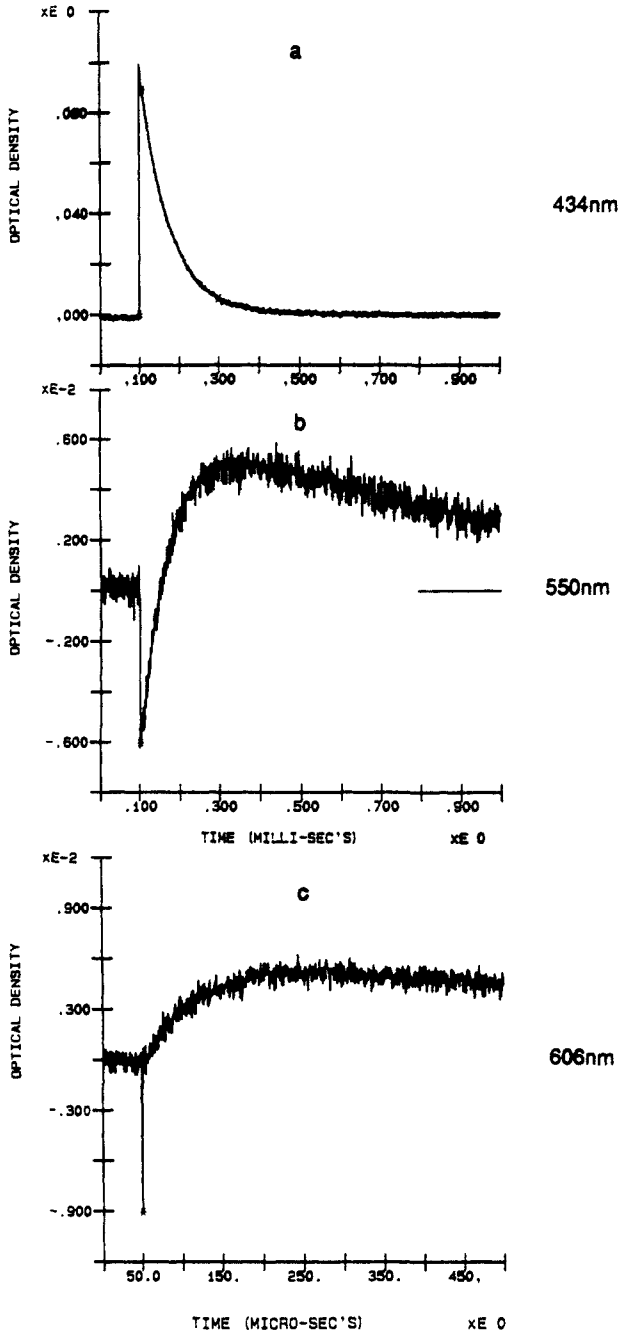

Figure 5. Typical transient absorbance changes: (a) triplet decay of Up at 434 nm (isosbestic point for cytc(II)/cytc(III)); (b) cytc(II) formation monitored at 550 nm (maximum absorbance change between cytc(II) and cytc(III)); (c) Up cation-radical formation monitored at 606 nm (isosbestic point for $^3Up^*/Up$). Conditions: [Up] = [cytc(III)] = 35 μM, at 25 °C, pH 7.26, and μ = 500 mM.

Table III. Fraction of Fast Triplet Decay Component (25 °C, pH 7.26, μ = 4 mM)

	[cyto] (μM)						
	15	25	30	35	42.5	50	65
f	0.40	0,64	0.74	0.82	0.89	0.93	0.96
$\Delta A_1/(\Delta A_1 + \Delta A_2)$ (%)	13.3	29.1	45.1	61.7	76.6	80.0	83.6

was present (up to 50 μM), the Up(T_1) absorbance was markedly reduced, the triplet lifetime was decreased, and the decay became nonexponential (Figure 7) but could be fitted by a two-exponential function of the form

$$f(t) = A \exp(-\gamma_1 t) + B \exp(-\gamma_2 t)$$

The slower component (γ_2) was found to be dependent upon [cytc(III)] in a qualitatively similar way to the T_1 behavior at high ionic strength (vide infra). The faster component (γ_1) showed a mean decay constant of (1.7 ± 0.4) × 10^6 s^{-1}, which was independent of cytc(III) concentration up to 50 μM, although the fractional contribution of γ_1 to the total decay increased with cytc(III) concentration—Table III.

Meanwhile, at 550 nm, we observed a rapid rise and subsequent decay of an absorbance (Figure 7), identified as cytc(II). Analysis

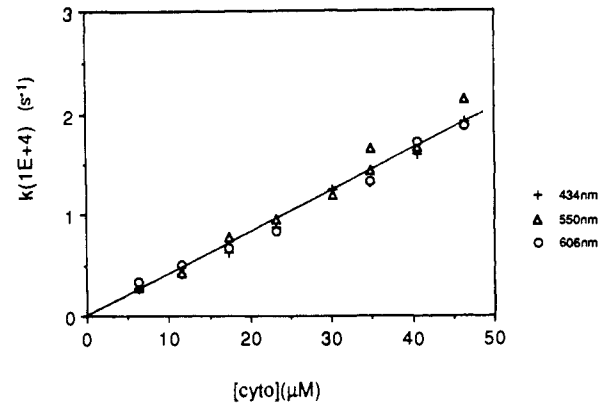

Figure 6. Rates of triplet decay and growth of electron-transfer products as a function of cytc(III) concentration (25 °C, pH 7.26, and 500 mM ionic strength in phosphate buffer): +, triplet decay at 434 nm; Δ, growth of reduced cytc; O growth of cation radical of porphyrin.

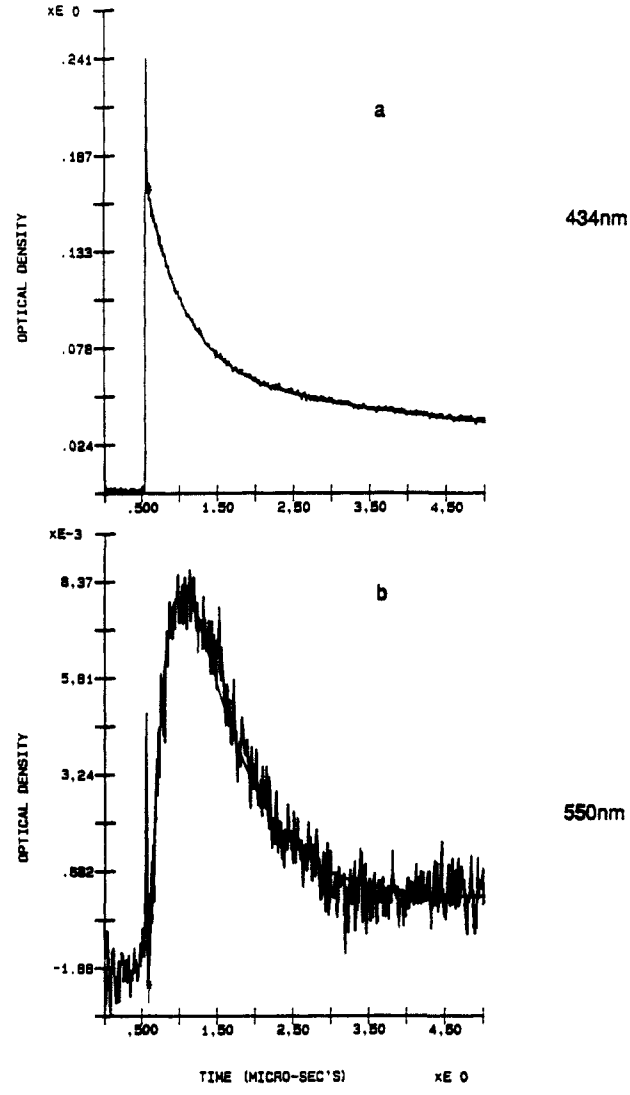

Figure 7. Transient kinetics of Up in the solution containing 35 μM Up and 35 μM cytc(III) (25 °C, pH 7.26, and 4 mM ionic strength in phosphate buffer): (a) decay of absorbance of Up(T_1) monitored at 434 nm; (b) decay of intermediate cytc(II) at 550 nm.

Table IV. Intramolecular Electron-Transfer Rate Constants and Redox Potentials (25 °C)

reaction	ΔE (V)	k (s^{-1})
Zncytc* + Fe^{III}Up → Zncytc$^+$ + Fe^{II}Up	0.45	(5.5 ± 0.8) × 10^5
ZnUp$^+$ + cytc(II) → ZnUp + cytc(III)	0.57	(8.5 ± 0.2) × 10^5
Up$^+$ + cytc(II) → Up + cytc(III)	0.60	(3.7 ± 0.6) × 10^6
^{3}Up* + cytc(III) → Up$^+$ + cytc(II)	1.06	(1.7 ± 0.3) × 10^6
^{3}ZnUp* + Cytc(III) → ZnUp$^+$ + cytc(II)	1.19	(2.0 ± 0.2) × 10^6
Zncytc$^+$ + Fe^{II}Up → Zncytc + Fe^{III}Up	1.23	(1.4 ± 0.1) × 10^4

by a double-exponential function showed the rising fragment to have a rate constant of 3.7 × 10^6 s^{-1}. The decaying portion showed a rate constant of 2 × 10^6 s^{-1}, equal to that of the γ_1 component of the T_1 decay. A spectral determination over the range 430–580 nm showed that both fast and slow components had identical spectra, i.e., that of the Up(T_1) state.

(2) Zinc(II) Uroporphyrin and Cytc(III). In a related set of experiments, Zn^{II}Up was prepared and excited to its T_1 level by a 532-nm laser flash. The resulting absorption at 434 nm decayed monoexponentially in deaerated aqueous buffer at pH 7.26 with a lifetime of 3.5 ms. When cytc(III) was added up to 30 μM, the T_1 decay became nonexponential as with Up(T_1). The data could be successfully fitted with a double-exponential: the faster component had a rate constant that was concentraton independent (k = 2.0 × 10^6 s^{-1}), and the slower component had a rate constant that varied with cytc(III) concentration in a first-order manner.

At 550 nm, where cytc(II) absorbs, the production and decay of a transient absorption were qualitatively similar to that shown in Figure 7b. The rate constants for the rise and fall of the cytc(II) state were 2.0 × 10^6 and 8.5 × 10^5 s^{-1}, again independent of cytc(III) concentration.

(3) Zn^{II}cytc and Iron(III) Uroporphyrin. In this couple we reverse the position of primary donor and acceptor. The zinc(II) derivative of cytc has a T_1 state that showed a lifetime of 10 ms in pH 7.26 buffer. In the presence of an increasing concentration of iron(III) uroporphyrin, the triplet decayed in a complex manner that was fit by a two-exponential fitting routine. As with the Zn^{II}Up/cytc(III) system, the decay of the fast component was independent of Fe^{III}Up concentration (5–30 μM) and was concomitant with the formation of a 428-nm absorption arising from Fe^{II}Up. This latter species decayed with a rate constant of 1.4 × 10^4 s^{-1}, which showed no dependence on Fe^{III}Up concentration.

The rate constants for all the forward and reverse electron-transfer reactions that we have measured are collected in Table IV.

Discussion

1. Absorbance and Fluorescence Data. The tandem cell experiments and the Job plot indicate that uroporphyrin and cytc(III) form a strong 1:1 complex at low ionic strength. Such self-association is found between cytochrome *c* and cytochrome *c* peroxidase,[25] cytochrome b_5,[35] and flavodoxin.[33] Table II shows how the association constant depends on ionic strength. Excitation of Up into the S_1 state by 612-nm irradiation leads to fluorescence that is quenched by the cytc at low ionic strengths. At μ = 500 nM, Up S_1 states are not quenched by cytc(III) up to 50 μM. Under these conditions, complex formation is negligible and the lack of fluorescence quenching indicates that diffusive processes are unable to cause Up(S_1) and cytc(III) to interact at concentration up to 50 μM. At such a concentration, with an assumed upper limit of a quenching constant of 10^{10} M^{-1} s^{-1}, a quenching rate of 5 × 10^5 s^{-1} is estimated, which is 2 orders of magnitude lower than the fluorescence lifetime of Up(S_1). Thus, it is no surprise that diffusional quenching of fluorescence is negligible.

The quenching at low ionic strengths, therefore, where complexation is significant, must arise from the formation of a porphyrin–protein couple in sufficient proximity for static quenching to occur. The generally upward curvature of the low ionic strength Stern–Volmer plots in Figure 4 supports this concept. However, we note that the 4 mM ionic strength plot in Figure 4 curves off again at high cytc(III) concentration. A plot of the integrated fluorescence intensities (F) vs [cytc(III)] levels out at a F value that is ca. 10% of that initially; i.e., the complex itself has residual fluorescence.

2. Triplet-State Data. a. High Ionic Strength. At high values of ionic strength (e.g., 500 mM) the behavior of Up(T_1) is straightforward and similar to that observed for meso-substituted tetraphenylporphyrins by Cho et al.[23] The porphyrin is effectively free in solution prior to the excitation pulse, and T_1 states interact with the protein solely through random diffusive encounters that are characterized by the following process:

$$\text{Up(aq)} \rightarrow {}^1\text{Up*(aq)} \quad (1)$$

$${}^1\text{Up*(aq)} \rightarrow \text{Up(aq)} + h\nu_F \quad (2)$$

$${}^1\text{Up*(aq)} \rightarrow {}^3\text{Up*(aq)} \quad (3)$$

$${}^3\text{Up*(aq)} + \text{cytc(III)} \rightarrow \text{Up}^+\text{(aq)} + \text{cytc(II)(aq)} \quad (4)$$

where Up$^+$ and cytc(II) represent the radical cation of uroporphyrin and the reduced form of cytochrome *c*, respectively. Reaction 4 yields freely diffusing species that undergo a bimolecular dismutation process over several milliseconds with the re-formation of the starting ground states. At 500 mM ionic strength, the plot of Figure 6 yields a rate constant of 4.1 × 10^8 M^{-1} s^{-1} for the forward electron-transfer step in reaction 4.

Measurements of the efficiency of cytc(II) formed per ^{3}Up* quenched showed reaction 4 to be only 22% efficient. This may be a consequence of the inability of the majority of the electron-transfer products to successfully escape the solvent cage in which they formed. That free Up$^+$ and free cytc(II) are formed

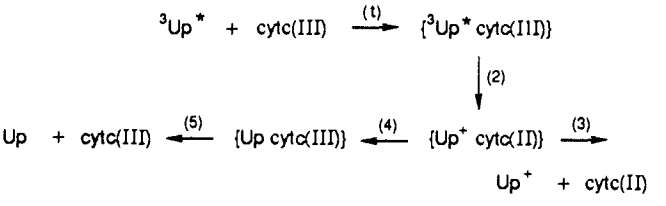

in such excellent concomitance (Figure 6) with the caged products {Up$^+$/cytc(II)} being kinetically invisible is most likely the consequence of the electron-transfer step (2) being much slower than any of the others in the sequence.

b. Low Ionic Strength. The situation becomes more interesting and less straightforward at μ = 4 mM. Now the initial triplet yield is greatly decreased, and the decay is not a single exponential. Table III shows how the triplet yield at zero time is partitioned into the fast- and slow-decaying components and how this ratio depends on cytc(III) concentration. Clearly, the higher the fraction complexed, the higher the relative yield of the rapid process. At 65 μM cytc(III) where 96% of the uroporphyrin is complexed, the total amount of T_1 state at t = 0 is only ca. 11% of that in the absence of cytc(III). This ties up with the residual fluorescence from ^{1}[Up/cytc(III)]* referred to earlier, again providing evidence that the deactivation to ground state in ^{1}[Up/cytc(III)]* does not totally dominate fluorescence and intersystem crossing.

Clearly two populations of triplet state exist that exhibit different decay properties. The slow component is identified as arising from Up T_1 states that are uncomplexed. This decay is dependent on cytc(III) concentration, and plots (Figure 8) of the decay rate vs the concentration of *uncomplexed* protein show excellent linearity with a slope that depends critically on the ionic strength (Figure 9). This phenomenon was well characterized by Cho et al.[23] for the meso-substituted porphyrins. These workers, however, did not observe the departures from monoexponentially found here. It may be that the different porphyrins used showed less complexing behavior, but it is clear from our observations that the triplet decay such as shown in Figure 7 is not a single expo-

(35) Mauk, M. R.; Reid, L. S.; Mauk, A. G. *Biochemistry* **1982**, *21*, 1843–1896.

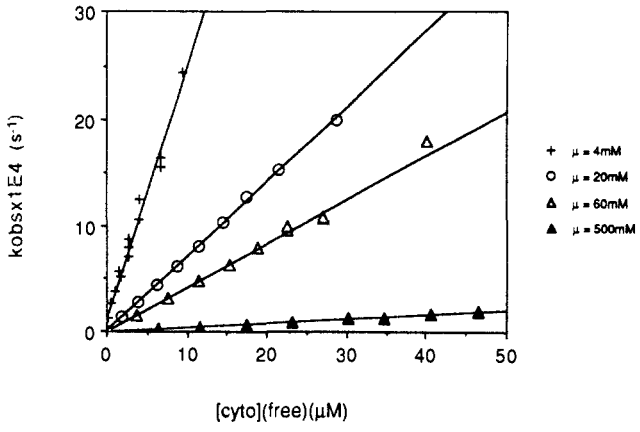

Figure 8. Triplet decay rate constants as a function of free cytochrome *c* concentration at pH 7.26 and 4, 20, 60, and (d) 500 mM ionic strengths, respectively. [Up] = 35 μM.

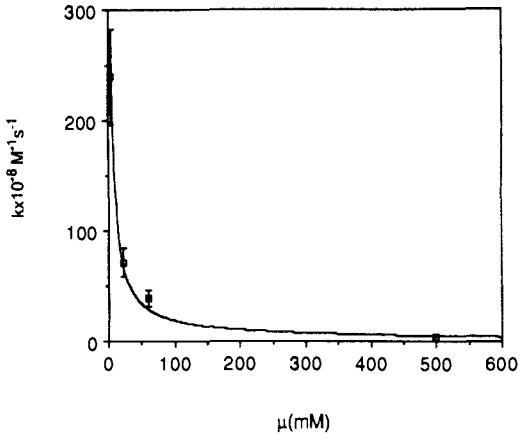

Figure 9. Bimolecular rate constants of Up triplet quenching by cytc(III) as a function of ionic strengths at pH 7.26 (phosphate buffer). The solid curve is that calculated from Debye–Hückel–Onsager theory.

nential but has the characteristics listed in Table III.[36]

The fast component, described here as Upcytc(T_1)—the triplet state of the complex—decays with a first-order rate constant of 1.9×10^6 s^{-1} independent of the cytc(III) concentration. Under the same conditions we note that the absorbance of the cytc(II) species at 550 nm grows with a concentration-independent rate constant of 3.7×10^6 s^{-1}; i.e., the reduced product grows in faster than its precursor (the triplet) decays. However, the reduced heme protein disappeared with a rate constant that parallels that of the T_1 decay. This behavior is consistent with the scheme

$$^3[\text{Up/cytc(III)}]^* \rightarrow [\text{Up}^+\text{/cytc(II)}] \rightarrow [\text{Up/cytc(III)}]$$

in which the first-order rate constants k_F and k_R are such that $k_R > k_F$. Analysis of the formation and decay of the cytc(II) absorbance at 550 nm allows the evaluation of k_R as the rapidly rising part in Figure 7 and k_F as the slower decaying part in the same figure. The value of k_F is also obtained from the fast segment of the T_1 decay (at 434 nm). The values of k_F and k_R were found to be the same at ionic strengths of 4 and 20 mM, which indicates that the electrolyte concentration has no influence on the conformation and intersite distance in the complex but simply governs the fraction of the complex present.

(36) A reviewer properly points out that we should anticipate observing an early bleaching transition in Figure 7 caused by immediate formation of porphyrin T_1, similar to that shown in Figure 5b for the high ionic strength case. At low cytc(III) concentrations where a significant amount of intermolecular reaction occurred, this was the case. At 35 μM cytc(III)—the condition for Figure 7—the complex accounted for 85% of the total cytc(III) present and the intermolecular component was weak. Triplet quantum yields are much lower under these conditions, and the consequent weak rapid bleaching became obscured by an intense scattered-light transient component at 550 nm, which is very close to the 532-nm excitation light.

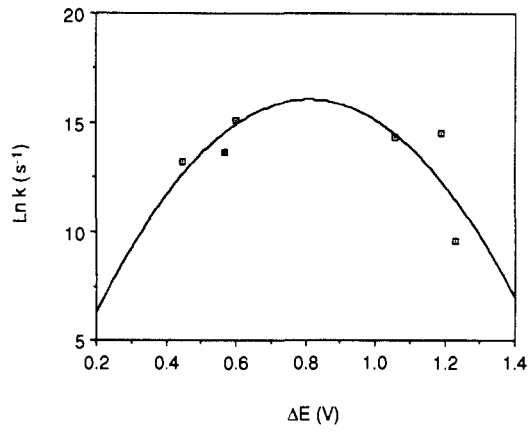

Figure 10. Rate constants of intramolecular electron transfer as a function of redox potentials. The solid line is a theoretical curve with $\lambda = 0.81$ V and $\ln(\nu k_E) = 14.80$.

Our experiments at high ionic strength (vide supra) showed that the Up T_1 state yielded only 22% ion pairs via the bimolecular process. This proved to be very different in the intramolecular case. For example, under comparable conditions we obtained $\Delta A_{550} = 0.0335$ and $\Delta A_{434} = 0.104$. The former value is obtained from fitting curves such as Figure 7 when the computer provides the total extent of the reduced cytochrome as if no decay occurred. The latter value is that derived from ΔA_{434} at $t = 0$ less that amount of free Up(T_1) produced. Earlier we stated that the ratio of the extinction coefficients of triplet to reduced cytochrome was 2.3. From this we find that the ratio of the concentrations of cytochrome *c*(II) to triplet is 0.74. Considering the errors in the extrapolation and the uncertainty about whether the molar extinction coefficients of the complex and free T_1 states are equal, we conclude that the intramolecular process is close to unit efficiency on the basis of the initial triplets.

c. Other Photoredox Couples. While we have not yet established through difference spectroscopy that the couples Zn^{II}Up/cytc(III) or Zncytc/Fe^{III}Up form ground-state self-association complexes, our observations of the triplet-state behavior at low ionic strength (4 mM) strongly indicate that such complexes are indeed formed by these systems that are electronically similar to the Up/cytc(III) system.

Thus, the triplet states (primary donors) decayed exponentially in the absence of acceptor species but decayed much more rapidly and nonexponentially when the acceptor was present at a low micromolar concentration level. This nonexponential behavior of the decay showed good double-exponential behavior, the first component of which increased in extent, but not in decay rate, as the acceptor concentration was increased, and its decay was a first-order function of the acceptor concentration.

Further, at the wavelengths where the singly reduced acceptor absorbed, our observations showed the formation of a reduced species concomitant with the fast decay of the donor triplet state. This in turn decayed in a back-transfer step.

Overall, this behavior is entirely consistent with forward and reverse electron transfer within porphyrin–protein complexes that are formed as a result of electrostatic association between the two entities. In the two systems referred to here, our data (Table IV) show that $k_F > k_R$, unlike the Up/cytc(III) couple.

The three porphyrin–protein complexes studied so far all yield k_F and k_R values that are tabulated along with driving force values (ΔE) in Table IV. We have plotted in Figure 10 the values of $\ln k$ against ΔE. An inverted parabola of the form in semiclassical electron-transfer theory[37]

$$\ln k = -(\Delta G^\circ + \lambda)^2/4\lambda RT + B \qquad B = \ln(\nu k_E) \quad \text{(A)}$$

fitted to the data points is shown superimposed. The λ parameter, according to semiclassical electron-transfer theory, is an energy quantity that comprises nuclear reorganization of reactants,

(37) Marcus, R. A.; Sutin, N. *Biochim. Biophys. Acta* **1985**, *811*, 265–322.

products, and their environment; λ represents the vertical separation between the product and reactant potential energy surfaces.

Expression A is only valid when the series of reactions under study is homogeneous, i.e., when λ and the electronic coupling factors k_E are invariant throughout the series. One important consideration in respect to the electronic factors is whether the intersite distance and conformation are constant throughout the three systems we have studied. We intend to examine this closely by energy-minimized modeling, nonradiative electronic transfer, and two-dimensional NMR experiments. However, for the moment we rely only on the surmise that the configuration of the complex is primarily set by the electrostatic interactions between the cationic lysines of the protein and the anionic groups on the uroporphyrin periphery and that differences in electron density at the metal centers are insignificant in governing the transfer distance. Such differences in electron density arise from the electron-transfer act itself and from substitution of different metals in the heme and uroporphyrin moieties. In this assumption we follow those who have investigated electron transfer in protein-protein associated systems[15-22] and those who covalently link transition-metal complexes to protein surface sites.[8-14]

On the strength, or weakness, of these assumptions we point out that λ = 0.81 V from our data is in line with the values estimated by McLendon and Miller[18] and by Conklin and McLendon[19] in their work on protein-protein complexes and by Meade, Gray, and Winkler[14] for the systems involving ruthenium modifications to cytochrome *c*. To date, all such reactions involving electron transfer into, or out of, a heme (or modified heme) protein show λ values near 1 eV.

In conclusion, we note that by adjusting the ionic strength in aqueous systems containing cytochrome *c* and a highly anionic porphyrin, such as uroporphyrin or its metallo derivatives, we can switch from a diffusional, bimolecular photoinduced electron-transfer process to one that occurs unimolecularly within a preformed electrostatically bound protein-porphyrin complex. In this we differ from Cho et al.[23] who reported only a diffusional type with related systems. Our system on the one hand is reminiscent of protein-protein self-associated complexes because the association of the units relies on electrostatic docking forces. On the other hand it resembles the covalently linked protein-Ru complex systems where one member of the couple is a small molecule located at the protein surface. As in these approaches, our system removes complications that result from diffusion. Perhaps the uroporphyrin/cytochrome *c* system offers an experimentally simpler approach. Further work on extending and refining Figure 10 is in progress.

Acknowledgment. This research has been supported in part by NIH Grant GM31603 and by the Center for Photochemical Sciences at Bowling Green State University. We are grateful to Professors F. Scandola and V. Balzani for useful discussions. We express our thanks particularly to Dr. W. E. Ford for his very useful help during the early stages of this project.

Registry No. Uroporphyrin, 26316-36-9.

Hydrazines: New Charge-Transfer Physical Quenchers of Singlet Oxygen

E. L. Clennan,* L. J. Noe,* E. Szneler, and T. Wen

Contribution from the Department of Chemistry, University of Wyoming, Laramie, Wyoming 82070. *Received December 14, 1989*

Abstract: The rates of reaction of singlet oxygen with 25 hydrazines were determined by following the emission of singlet oxygen at 1270 nm as a function of time. These data are utilized to discuss various options for the quenching mechanism including electron transfer, electronic to vibrational energy transfer, and a contact charge-transfer process.

It is now well established that singlet oxygen is responsible for photodynamic destruction of both biologically and commercially important molecules. As a consequence, it is of some practical importance to search for and to investigate the properties of molecules capable of physically quenching[1] this reactive species. Molecules that have been identified as physical quenchers of singlet oxygen include amines,[2] sulfides,[3] carotenoids,[4] metal chelates,[1b] nitroxides,[1b] phenols,[1b] inorganic anions,[1b] and nitroso compounds.[1b]

It has been recognized that physical quenching of $^1O_2$ occurs by four distinctly different mechanisms:[1a] (an energy-transfer mechanism (for example, carotenoids have low-lying excited states capable of accepting the energy from the $^1\Delta_g$ state of O_2); (2) a reactive quenching mechanism that involves covalent bonding of $^1O_2$ to a substrate followed by decomposition to triplet oxygen

Chart I

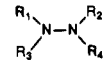

1. $R_1 = R_2 = R_3 = R_4 = Me$
2. $R_1 = R_2 = R_3 = R_4 = iBu$
3. $R_1 = R_2 = Me$; $R_3 = R_4 = Et$
4. $R_1 = R_2 = Me$; $R_3 = R_4 = nPr$
5. $R_1 = R_2 = Me$; $R_3 = R_4 = nBu$
6. $R_1 = R_2 = Me$; $R_3 = R_4 = nPe$
7. $R_1 = R_2 = Me$; $R_3 = R_4 = iBu$
8. $R_1 = R_2 = Me$; $R_3 = R_4 = neoPe$
9. $R_1 = R_2 = R_3 = Me$; $R_4 = iBu$
10. $R_1 = R_2 = R_3 = Me$; $R_4 = neoPe$
11. $R_1 = R_3 = Me$; $R_2 = R_4 = iBu$
12. $R_1 = R_3 = Me$; $R_2 = R_4 = neoPe$
13. $R_1 = R_2 = R_3 = R_4 = CD_3$

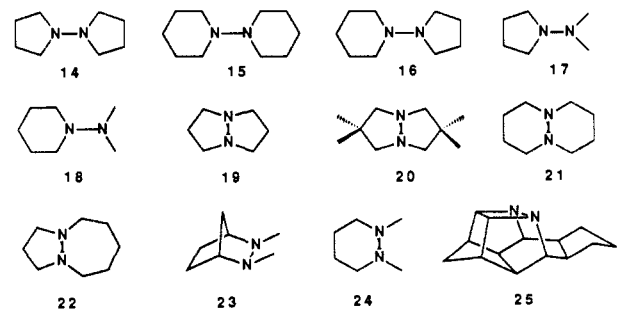

14 15 16 17 18 19 20 21 22 23 24 25

(1) (a) Foote, C. S. In *Singlet Oxygen*; Wasserman, H. H., Murray, R. W., Eds.; Academic Press: New York, 1979; p 139. (b) Bellus, D. In *Advances in Photochemistry*; Pitts, J. N., Hammond, G. S., Gollnick, K., Eds.; John Wiley and Sons: New York, 1979; Vol. 11, p 105.

(2) (a) Ouannes, C.; Wilson, T. *J. Am. Chem. Soc.* **1968**, *90*, 6527. (b) Ogryzlo, E. A.; Tang, C. W. *J. Am. Chem. Soc.* **1970**, *92*, 5034. (c) Young, R. H.; Martin, R. L. *J. Am. Chem. Soc.* **1972**, *94*, 5183. (d) Smith, W. F., Jr. *J. Am. Chem. Soc.* **1972**, *94*, 186. (e) Young, R. H.; Martin, R. L.; Feriozi, D.; Brewer, D.; Kayser, R. *Photochem. Photobiol.* **1973**, *17*, 233. (f) Monroe, B. M. *J. Phys. Chem.* **1977**, *81*, 1861. (g) Saito, I.; Matsuura, T.; Inoue, K. *J. Am. Chem. Soc.* **1981**, *103*, 188. (h) Manring, L. E.; Foote, C. S. *J. Phys. Chem.* **1982**, *86*, 1257. (i) Saito, I.; Matsuura, T.; Inoue, K. *J. Am. Chem. Soc.* **1983**, *105*, 3200.

(3) (a) Jensen, F.; Foote, C. S. *J. Am. Chem. Soc.* **1987**, *109*, 1478. (b) Nahm, K.; Foote, C. S. *J. Am. Chem. Soc.* **1989**, *111*, 1909. (c) Ando, W.; Takata, T. In *Singlet Oxygen*; Reaction Modes and Products. Part 2; Frimer, A. A., Ed.; CRC Press: Boca Raton, 1985; Vol. III, p 1.

(4) (a) Foote, C. S.; Denny, R. W. *J. Am. Chem. Soc.* **1968**, *90*, 6233. (b) Foote, C. S.; Chang, Y. C.; Denny, R. W. *J. Am. Chem. Soc.* **1970**, *92*, 5216.

0002-7863/90/1512-5080$02.50/0